Navigation Systems May Deteriorate Stability in Traffic Networks

Gianluca Bianchin and Fabio Pasqualetti

Abstract— **Advanced traffic navigation systems, which provide routing recommendations to drivers based on real-time congestion information, are nowadays widely adopted by roadway transportation users. Yet, the emerging effects on the traffic dynamics originating from the widespread adoption of these tools have remained largely unexplored until now. In this paper, we propose a dynamic model where drivers imitate the path preferences of previous drivers, and we study the properties of its equilibrium points. Our model is a dynamic generalization of the classical *traffic assignment framework*, and extends it by accounting for dynamics both in the path decision process and in the network's traffic flows. We show that when travelers learn shortest paths by imitating other travelers, the overall traffic system benefits from this mechanism and transfers the maximum admissible amount of traffic demand. On the other hand, we demonstrate that when the travel delay functions are not sufficiently steep or the rates at which drivers imitate previous travelers are not adequately chosen, the trajectories of the traffic system may fail to converge to an equilibrium point, thus failing asymptotic stability. Illustrative numerical simulations combined with empirical data from highway sensors illustrate our findings.**

I. INTRODUCTION

Roadway traffic networks are fundamental components of modern societies, making economic activity possible by enabling the transfer of passengers, goods, and services in a timely and reliable fashion. Despite their critical role, these transportation systems are impaired by the long-standing problem of traffic congestion, which wastes billions of gallons of fuel each year [1], [2]. Advanced navigation systems are nowadays widely adopted by travelers, largely thanks to the widespread use of smartphone-based navigation apps (such as Google Maps, Inrix, Waze, Apple Maps, etc.) [3]. Advanced navigation systems provide shortest-path routing recommendations based on real-time global travel time information. On the one hand, these technologies have enabled travelers to save time and fuel but, on the other hand, they have transformed the transportation infrastructure originating unanticipated effects and disrupting existing traffic flow patterns [4]. While the implications of the widespread adoption of advanced navigation systems have been analyzed game-theoretically [5], a characterization of the impact of these technologies on dynamic models of traffic for general, dynamic, traffic networks has remained elusive until now.

In this work, we study the stability properties of a traffic system composed of the interconnection between a dynamic model of traffic flows (inspired from the Cell Transmission Model [6]) and a dynamic model of route selection (derived from the Replicator Dynamics [7]). Our choice of using the replicator equation is motivated by recent studies that showed that this model emerges as an aggregate description of learning processes in large populations and as the limiting case of the best response dynamics [8]. We show that, at equilibrium, our model shares the same properties as the well-studied routing game [5], and thus it is consistent with existing studies that focus on systems operating at equilibrium. It is worth noting that, with respect to the classical routing-game framework, our model accounts for dynamics both in the *route selection process* as well as in the *traffic flow model.* Our dynamical model suggests that systems where travelers continuously prefer highways with minimal latency to destination – and select these highways by imitating other travelers already in the network – admit an equilibrium point provided that the external inflow is bounded above by the min-cut capacity. This implies that traffic systems where the users learn through imitation transfer the maximum amount of flow that is transferable by a network operating at equilibirum. This connects our work with classical static flow models used in the transportation literature. Moreover, our results show that when the rate of imitation (namely, the frequency at which new users imitate the path preferences of other users) is either too small or too large, the equilibrium points may fail to be asymptotically stable, thus implying that in unregulated networks the congestion state may oscillate around (or escape from) the equilibria.

Related Work. The traffic model proposed here finds its roots in the well-established routing game [9] and corresponding traffic assignment problem [5], which have been used in the transportation literature to model how travelers make decisions in congested traffic. Recently, this framework has received increased attention with several studies investigating the impact of different sources of information on the traffic system; e.g., see [10]–[13] and the references therein. One of the main limitations of this classical approach is that it models systems operating at equilibrium, thus neglecting dynamics near these points. For this reason, evolutionary dynamics [7] have been proposed to study the dynamic properties of equilibria [14], [15]. Although these works represent a step forward toward understanding the impact of advanced navigation systems on traffic patterns, the used models still rely on *static descriptions,* where traffic flows propagate instantaneously across the network. It is immediate to realize that such models are accurate only when the routing preferences update at a *slower timescale* than that of the traffic dynamics (e.g., when drivers update their path preferences from day-to-day as a result of a personal observation) On the other hand, in modern traffic networks, advanced navigation systems allow drivers to update their routing preferences *at the same timescale* as the traffic flows, thanks to real-rime traffic state measurements. This connects our work with the body of literature on dynamic traffic flow models. Our model is a continuous-time version of the Cell-Transmission Model [6] and related to the model studied in [16]. Dynamic traffic models with static routing preferences have been studied in [17] using monotonicity, in [18] using mixed monotonicity, in [19] using passivity. Of particular relevance to the framework studied here are [17], [20]. With respect to these works, here we study path selection mechanisms governed by the replicator equation and we focus on the game-theoretic properties of this model and its stability analysis. This work extends the preliminary work of the authors [19] in several directions, including a formal proof of uniqueness and evolutionary stability of the Nash equilibrium, and a sufficient condition to ensure asymptotic stability of the equilibrium point. Finally, the recent works [21], [22] also highlighted detrimental effects of navigation systems in a small-scale (two-link) network.

Contribution. The contribution of this work is threefold. First, we propose a dynamic model derived from the replicator dynamics to describe the path selection mechanism underlying drivers' decisions in congested traffic. We then couple this routing model with a dynamic model of traffic, which describes the evolution of traffic flows in the network in relation to the instantaneous routing choices. Relative to the classical traffic assignment framework, the use of a dynamic traffic model describes modern networks where *routing decisions and traffic flows update at the same timescale.* As illustrated in Section V, this model allows us to capture dynamic behaviors observed in practice, which could not be explained using static models [23], [24]. Second, we study the game-theoretic properties of the equilibria of the interconnected model. We show that, under suitable assumptions, an equilibrium point exists, is unique, and coincides with an evolutionary stable Nash (or Wardrop) equilibrium [25]. This relates our work with the well-established routing game [9]. Third, we study the stability properties of the equilibrium. By using a Lyapunov-based reasoning, we derive sufficient conditions under which the equilibrium is asymptotically stable. In simulation, we show that the conditions are tight and that oscillating trajectories can emerge when our conditions do not hold. Intuitively, oscillations originate because the population is overreacting to small changes in congestion, more precisely, in practice this occurs because individual users update their routing preferences without anticipating the preferences of the rest of the population. This behavior is consistent with field data (see, e.g., [23], [24]).

Organization. This paper is organized as follows. Section II presents the proposed model. Section III derives conditions for existence and uniqueness of an equilibrium point and in Section IV we study the stability properties of the equilibria. Section V illustrates our findings via numerical simulations and Section VI concludes the paper.

Notation. Given $x \in \mathbb{R}^n, u \in \mathbb{R}^m$, we let $(x,u) \in \mathbb{R}^{n+m}$ denote their concatenation; if $n=m$, $\langle x, u\rangle$ denotes the inner product. For symmetric matrix M, $\lambda_{\max}(M)$ and $\lambda_{\min}(M)$ denote its largest and smallest eigenvalue, respectively.

II. Model of traffic network

In this section, we present our models of traffic flows and routing decisions, and we formalize the problem we study.

A. *Traffic flow model*

We model a transportation network using a digraph $\mathcal{G} = (\mathcal{V}, \mathcal{E})$, where $\mathcal{V}$ is the set of nodes and $\mathcal{L}$ is the set of links. In what follows, we let $\mathcal{L} = \{1, \dots n\}, n \in \mathbb{N}_{>0}$. For a link $i \in \mathcal{L}$, we denote by $o_i \in \mathcal{V}$ its origin node and by $d_i \in \mathcal{V}$ its destination node. Motivated by real-world transportation networks with parallel highways, we will allow for parallel links, namely, we admit $i, j \in \mathcal{L}$ such that $i \neq j$ and have the same origin and destination: $o_i = o_j$ and $d_i = d_j$. A *path* in $\mathcal{G}$ is a sequence of links $\{i_1, i_2, \dots\}$ such that the origin node of each link is the destination node of the preceding one. Notice that a path may contain repeated links and, going along the path, one may reach repeated nodes. A path is *simple* if it does contain the same link more than once. The *length* of a path is the number of edges contained in $\{i_1, i_2, \dots\}$. Following the Cell Transmission Model [6], we describe the macroscopic behavior of traffic on each link $i \in \mathcal{L}$ over time $t \geq 0$ using the conservation law:

$$\dot{x}_i(t) = f_i^{\text{in}}(x(t)) - f_i^{\text{out}}(x(t)), \tag{1}$$

where $x_i(t) \in \mathbb{R}$ is the traffic density in link i, $f_i^{\text{in}}(x(t))$ is the traffic inflow entering at upstream, and $f_i^{\text{out}}(x_i(t))$ is the traffic outflow exiting at downstream. We make the following assumptions on the outflow functions.

Assumption 1: For all $i \in \mathcal{L}$, the outflow function $f_i^{\text{out}}(x)$ depends only on the density x_i, namely, $f_i^{\text{out}}(x) = f_i(x_i)$. Moreover, $f_i : \mathbb{R}_{\geq 0} \to \mathbb{R}_{\geq 0}$ satisfies $f_i(x_i) = 0$ if and only if $x_i = 0$, it is continuous, and strongly monotone; namely,

$$(x_i - \bar{x}_i)(f_i(x_i) - f_i(\bar{x}_i)) \geq \mu |x_i - \bar{x}_i|^2, \tag{2}$$

for some $\mu > 0$ and for all $x_i, \bar{x}_i \in \mathbb{R}_{\geq 0}$. □

We discuss this assumption in Remark 2.1 and we illustrate some choices of outflow functions in Example 2.2.

Assumption 1 guarantees that (1) is a positive system [26], namely, for every non-negative initial state and every non-negative input at all times, its state trajectory is non-negative. In what follows, for all $i \in \mathcal{L}$, we let

$$C_i := \sup_{z \in \mathbb{R}} f_i(z),$$

and $C = (C_1, \dots, C_n)$. If $f_i(\cdot)$ is unbounded, $C_i = +\infty$.

*Remark 2.1 (**Validity of Assumption 1**)***:** It is known (see, e.g., [16]) that the assumption that $f_i(x_i)$ only depends on x_i and is strictly increasing is valid provided that we restrict our focus to free-flow regimes [6]. More precisely, it has been shown in [16] that the free-flow equilibrium points of a more complete traffic model (that accounts for congestion regimes and backpropagation through the junctions) inherit the same stability properties of the model considered here. Hence, the conclusions drawn here will be applicable also to more complete models, provided that their operation is restricted to the free-flow regimes [16]. While we acknowledge that accounting for congested regimes is an important problem, due to the technical challenges in dealing with a more complete model, we leave a generalization of our framework as the focus of future works. Regarding the condition $f_i(x_i) = 0$ if and only if $x_i = 0$, the "if" part ensures that no vehicle density can flow out of a link when there is no density on it, and the "only if" part guarantees that any density is allowed to exit. □

*Example 2.2 (**Flow functions that satisfy Assumption 1**)*: A class of functions satisfying Assumption 1 (and used in, e.g., [27]) is that of linear outflow functions, given by

$$f_i^{\text{out}}(x_i) = \alpha_i x_i, \qquad \alpha_i > 0.$$

In this case, $C_i = +\infty$ and $\mu = \min\{\alpha_i\}_{i \in \mathcal{L}}$. A second class of functions satisfying Assumption 1 and used in [28] is

$$f_i^{\text{out}}(x_i) = C_i(1 - e^{-\beta_i x_i}), \qquad \beta_i > 0,$$

which is strongly monotone on any bounded set. □

Throughout this paper, we will focus on single-commodity networks, namely, networks for which there is a single origin node o where exogenous traffic flows enter the network, and a single destination node d, where flows exit the network. We assume that $\mathcal{G}$ is outflow-connected, namely, there is a path in $\mathcal{G}$ from every $i \in \mathcal{L}$ to d. To avoid trivial cases, we will also assume that there exists at least one path from o to d. We denote by $\lambda \in \mathbb{R}_{>0}$ the commodity inflow rate at o.

To model mass propagation through the nodes, we introduce the scalar routing ratios (or routing splits)

$$\{r_{ij}(t)\}_{i,j \in \mathcal{L}}, \qquad t \geq 0,$$

where $r_{ij}(t)$ models the fraction of flow exiting link i that proceeds toward j. We let $r_{ij}(t)$ be normalized fractions, so that $r_{ij}(t) \in [0, 1]$. Because exchange of flow is allowed only between consecutive links in the network, we have $r_{ij}(t) > 0$ only if $d_i = o_j$. Finally, mass is conserved through the nodes when $\sum_j r_{ij}(t) = 1$. Similarly, we let $r_{oi}(t) \in [0, 1]$ be the fraction of exogenous inflow λ that is routed from the origin node o to link i; analogously, we have $r_{oi}(t) = 0$ if $o_i \neq o$, and $\sum_{i \in \mathcal{L}} r_{oi} = 1$. In what follows, it will be useful to combine the network routing ratios into a matrix $R(t) = [r_{ij}(t)] \in \mathbb{R}^{n \times n}$ and the routing ratios at the origin into a vector $R_o = (r_{o1}, \ldots, r_{on}) \in \mathbb{R}^n$. See Example 2.4 for an illustration of the model and notation.

*Remark 2.3 (**Temporal dependence in the routing ratios**)*: In this discussion, we treated $\{r_{ij}(t)\}_{i,j \in \mathcal{L}}$ as time-varying quantities; we will see shortly below (cf. Section II-B) that the time-dependency in $r_{ij}(t)$ implicitly originates as a function of the traffic state $x(t)$. □

At every node of $\mathcal{G}$, traffic flows are conserved, and thus the inflow to each link $i \in \mathcal{L}$ is given by

$$f_i^{\text{in}}(x) = r_{oi}(t)\lambda + \sum_{j \in \mathcal{L}} r_{ji}(t) f_j(x_j(t)).$$

By substituting into (1), the density on each link evolves as:

$$\dot{x}_i(t) = r_{oi}(t)\lambda + \sum_{j \in \mathcal{L}} r_{ji}(t) f_j(x_j(t)) - f_i(x_i(t)). \tag{3}$$

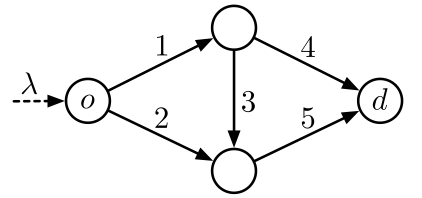

Fig. 1: Graph topology used to illustrate our model. See examples 2.4 and 2.6. Nodes labeled by 'o' and 'd' describe the origin and destination, where exogenous inflows enter and exit the network, respectively. The dashed arrow illustrates the exogenous inflow.

By letting

$$x := (x_1, \ldots x_n), \qquad f(x) := (f_1(x_1), \ldots, f_n(x_n))$$

be the joint vectors of densities and flows, respectively, the network state evolves according to:

$$\dot{x}(t) = (R(t)^\mathsf{T} - I) f(x(t)) + R_o(t)\lambda. \tag{4}$$

We illustrate this traffic model in Example 2.4.

*Example 2.4 (**Illustration of traffic flow model**)*: Consider the network topology in Fig. 1. The model (4) reads as:

$$\begin{aligned}
\dot{x}_1 &= -f_1(x_1) + r_{o1}\lambda, & \dot{x}_3 &= -f_3(x_3) + r_{13} f_1(x_1), \\
\dot{x}_2 &= -f_2(x_2) + r_{o2}\lambda, & \dot{x}_4 &= -f_4(x_4) + r_{14} f_1(x_1), \\
\dot{x}_5 &= -f_5(x_5) + f_2(x_2) + f_3(x_3), & &
\end{aligned}$$

where time dependencies have been dropped for compactness. Notice that the routing ratios satisfy $r_{o1} + r_{o2} = 1, r_{13} + r_{14} = 1$. □

B. Congestion-responsive path selection model

We next propose a model to describe the path selection process followed by drivers that seek to minimize their travel time to destination. Let $\mathcal{P}$ denote the set of simple paths from o to d. We assume that when a vehicle driver (hereafter called a user) enters the network at o, they select a path in $\mathcal{P}$, and they follow this path to destination without updating it while traversing the network. To model this process, we introduce the variables $\{y_p(t)\}_{p \in \mathcal{P}}$, where $y_p(t)$ denotes the fraction of exogenous inflow λ that is routed through path p at time t. We stress that $y_p(t)$ models a virtual amount of flow that may never be observed in the network: indeed, $y_p(t)$ describes the fraction of λ that is routed through p at time t, but the actual traffic flows on the links of p will be determined by the traffic flow model, as described shortly below. Hence, in what follows, we call $y_p(t)$ *demanded path flow* for path p (for a discussion on this wording choice, see Remark 2.7 shortly below). See Fig. 2 for an illustration. Then, the set of admissible path flow demands is the scaled simplex:

$$\Delta := \{y \in \mathbb{R}^p_{\geq 0} : \sum_{p \in \mathcal{P}} y_p = \lambda\}. \tag{5}$$

For link $i \in \mathcal{L}$, we let

$$y_i^l(t) := \sum_{p \in \mathcal{P} : i \in p} y_p(t), \tag{6}$$

be the *demanded link flows*. Similarly to the demanded path flows, the demanded link flow $y_i^l(t)$ describes the fraction of λ that is routed through link i at time t. In vector form, $y(t) = (y_1(t), \dots, y_{|\mathcal{P}|}(t))$ and $y^l(t) := (y_1^l(t), \dots, y_n^l(t))$. Notice that [5, Thm 2.2] guarantees that for any $y(t) \in \Delta$, $y^l(t)$ is uniquely determined.

To every link $i \in \mathcal{L}$, we associate a latency function $\ell_i^l(x_i)$ mapping traffic density into latency, and describing the travel time or latency required to traverse that link. With this notation, the total *demanded traffic latency* for path p is given by the sum of latencies of the links in that path:

$$\ell_p(x) := \sum_{i \in p} \ell_i^l(x_i). \tag{7}$$

In vector form, $\ell(x) := (\ell_1(x), \dots, \ell_{|\mathcal{P}|}(x))$ and $\ell^l(x) := (\ell_1^l(x_1), \dots, \ell_n^l(x_n))$. Motivated by [29], we make the following assumption on the latency functions.

Assumption 2: For all $i \in \mathcal{L}$, $\ell_i^l : \mathbb{R}_{\geq 0} \to \mathbb{R}_{\geq 0}$ is non-negative, continuous, and such that

$$\lim_{x_i \to f_i^{-1}(C_i)} \ell_i^l(x_i) = +\infty. \tag{8}$$

□

Assumption 2 is very mild, as it requires that every link has a non-negative travel time that varies smoothly as a function of the traffic densities and that tends to infinity as the link flow approaches the flow capacity; we refer to [29] for a detailed discussion on the validity of this assumption.

We consider a model where the vector of path preferences $y(t)$ is continuously updated over time based on the traffic state of the network. We adopt a model of path selection where the preference for a certain path $p \in \mathcal{P}$ will increase or decrease depending on whether that path has a better or worse travel time *compared to the network average*. To this end, we model the time-evolution of the flow demands using the replicator dynamics [30]:

$$\dot{y}_p(t) = y_p(\bar{\ell}(x(t), y(t)) - \ell_p(x(t))), \tag{9}$$

where

$$\bar{\ell}(x(t), y(t)) = \lambda^{-1} \sum_{p \in \mathcal{P}} y_p(t) \ell_p(x(t)), \tag{10}$$

is the average latency of traversing the network from o to d. Equation (9) states that the growth rate of flow demand for path p is proportional to the difference between the average latency of traversing the network $\bar{\ell}_p(x(t))$ and the latency of that path $\ell_p(x(t))$. We motivate our choice of adopting the replicator dynamics in Remark 2.5; we also note that this model has been widely adopted in the transportation literature to study dynamics in the routing game [14], [31].

Remark 2.5 (***Choice of the replicator dynamics***)**:** The replicator equation is a deterministic model of imitation, where future path preferences are selected by imitating successful path preferences of previous users. Replicator dynamics have originated in biology, arising in the study of animal behavior and evolution, and researchers later proved that this model is also an accurate description of

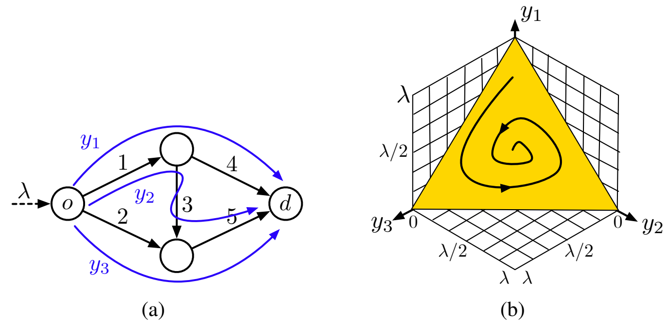

Fig. 2: (a) Demanded path flows: $y_1(t), y_2(t), y_3(t)$ describe the fraction of λ that is routed through paths, respectively, p_1, p_2, p_3 at time t. (b) The demanded path flows follow a model of path selection (cf. (9)) where the preference for a certain path will increase or decrease depending on whether that path has a better or worse travel time *compared to the network average*.

processes governed by machine learning algorithms in large populations [8]. Interestingly, this is a good model to describe the outcome of machine learning processes as its dynamics hinge on historical data and the paradigm of imitation (i.e., users observe others' travel times and change their own strategies based on these observations). Although our analysis is tailored to the replicator model, other selection models could be also considered – such as the best-response dynamics [32]. It is worth noting that the asymptotic properties of the trajectories are common across several different models of selection: for instance, [32] showed that noisy versions of the best-response dynamics have the same qualitative properties as the replicator dynamics. □

Example 2.6 (***Illustration of the path selection model***)**:** Consider the network illustrated in Fig. 5 and discussed in Example 2.4. This graph includes three simple paths $\mathcal{P} = \{p_1, p_2, p_3\}$ (see Fig. 2(a)) given by

$$p_1 = (1, 4), \qquad p_2 = (1, 3, 5), \qquad p_3 = (2, 5).$$

The demanded path flows y_1, y_2, y_3 are scalar quantities that model the fraction of exogenous inflow λ that is routed through, respectively, paths p_1, p_2, p_3. According to (6), the demanded flows on the links $y_1^l, y_2^l, y_3^l, y_4^l, y_5^l$ can be computed from the demanded flows on the path as follows:

$$y_1^l = y_1 + y_2, \quad y_2^l = y_3 \quad y_3^l = y_2, \quad y_4^l = y_1, \quad y_5^l = y_2 + y_3.$$

In words, the above relationships state that the flow on each link is the sum of the flows on paths passing through that link. The demanded traffic latencies of the paths (7) are

$$\ell_1(x) = \ell_1^l(x_1) + \ell_4^l(x_4), \qquad \ell_3(x) = \ell_2^l(x_2) + \ell_5^l(x_5),$$
$$\ell_2(x) = \ell_1^l(x_1) + \ell_3^l(x_3) + \ell_5^l(x_5).$$

Namely, the latency of each path is the sum of latencies of all links that compose that path. The average latency of traversing the network (10) is:

$$\bar{\ell}(x, y) = \lambda^{-1}(y_1 \ell_1(x) + y_e \ell_2(x) + y_3 \ell_3(x)),$$

and models the latency required to traverse the network, averaged over all paths. The replicator model (9) proposed to describe the path selection process in this case reads as:

$$\dot{y}_1 = y_1(\bar{\ell}(x,y) - \ell_1(x)), \qquad \dot{y}_2 = y_2(\bar{\ell}(x,y) - \ell_2(x)),$$
$$\dot{y}_3 = y_3(\bar{\ell}(x,y) - \ell_3(x)).$$

In words, the preference of users for a certain path grows proportionally to the difference between the average delay in the network the delay of that path. See Fig. 2(b). □

It is important to recall some important properties of the replicator model (9) that will be used throughout this paper. First, (9) satisfies $\sum_{p\in\mathcal{P}} \dot{y}_p(t) = 0$ at all times, and thus the simplex Δ is forward invariant. Namely, if $y(0) \in \Delta$, then, $y(t) \in \Delta$ for all $t > 0$. Second, the boundary faces

$$\mathrm{bf}_p\Delta := \{y : \sum_{p\in\mathcal{P}} y_p = \lambda, y_i = 0\}, \qquad p \in \mathcal{P},$$

are also forward invariant, and so are the boundary $\mathrm{bd}\Delta$ (i.e., the union of all the boundary faces) and the interior $\mathrm{int}\Delta$ (the subset satisfying $y_i > 0\ \forall i$). It is worth noting that, if $y(0) \in \mathrm{int}\Delta$, the trajectories of (9) may converge to the boundary only for $t \to +\infty$ and are confined to $\mathrm{int}\Delta$ for all finite t.

Importantly, these properties imply that if the initial condition $y(0)$ is such that $y_p(0) \in \mathrm{bf}_p$ for some $p \in \mathcal{P}$, the replicator equation will ignore y_p (namely, $y_p(t) = 0$ for all $t \geq 0$). This fact implies that one can define a new set of $|\mathcal{P}| - 1$ dimensional dynamics (9) where the variable y_p is removed, and the trajectories of the $|\mathcal{P}|$ dimensional and $|\mathcal{P}| - 1$ dimensional dynamics coincide at all times with the additional condition $y_p(t) = 0$ for all $t \geq 0$. Motivated by this observation, in what follows it will be convenient to restrict the state space Δ of (9) to the sub-simplex Δ' given by the support of the vector of initial conditions $y(0)$:

$$\Delta' := \{y \in \mathbb{R}^p_{\geq 0} : \sum_{p\in\mathcal{P}} y_p = \lambda, y_p = 0\ \forall p : y_p(0) = 0\}. \tag{11}$$

C. Combined model of traffic with congestion-responsive routing

In this section, we connect the traffic flow model (4) with the path selection model (9) to derive a model of traffic network with congestion-responsive routing. The key observation to relate the two models is that the set of demanded link flows $y(t)$ implicitly determines the routing ratios $r_{ij}(t)$, as described next. For a link $j \in \mathcal{L}$, let $\theta_j := \sum_{i\in\mathcal{L}:o_i=o_j} y_i^l$ denote the total demanded flow flowing through its origin node o_j. Then, given $y \in \Delta'$, we let the routing ratios depend on the demanded traffic flows as follows:

$$r_{ij}(y) = \begin{cases} 0 & \text{if } o_j \neq d_j, \\ y_j^l/\theta_j & \text{if } o_j = d_i \text{ and } \theta_j > 0, \\ \frac{1}{|\{k\in\mathcal{L}:o_k=o_j\}|} & \text{otherwise,} \end{cases} \tag{12}$$

where y_j^l is implicitly obtained from y using (6). The model (12) states that the outflow exiting link i splits among the available downstream links proportionally to the total flow demand on each downstream link, provided that each downstream link carries a nontrivial amount of flow, and is split uniformly among the downstream links otherwise. Notice that other allocation rules may be considered (e.g., where splits are non-uniform when $\theta_j = 0$).

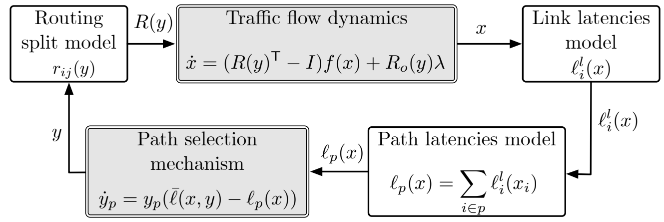

Fig. 3: The proposed model couples a compartmental-like model of traffic flows (see *"Traffic flow physics"*) with an economic model of route selection (see *"Path selection mechanism"*). Grey-shaded blocks illustrate dynamic models while white blocks illustrate algebraic relationships.

By combining (4), (7), (9), and (12) we obtain the following joint traffic flow model with congestion-responsive routing:

$$\dot{x}(t) = T(x(t), y(t)), \tag{13a}$$
$$\dot{y}(t) = F(x(t), y(t)), \tag{13b}$$

where $T : \mathbb{R}^n_{\geq 0} \times \Delta' \to \mathbb{R}^n, F : \mathbb{R}^n_{\geq 0} \times \Delta' \to \mathbb{R}^p$, are defined entry-wise, for all $i \in \{1, \ldots, n\}$ and $p \in \mathcal{P}$, as:

$$T_i(x,y) = r_{oi}(y)\lambda + \sum_{j\in\mathcal{L}} r_{ji}(y) f_j(x_j) - f_i(x_i),$$
$$F_p(x,y) = \eta\, y_p(\bar{\ell}(x,y) - \ell_p(x)).$$

Here, scalar $\eta > 0$ is a design parameter that we have introduced to modify the rate at which path preferences are updated. When the equation (13b) describes the behavior of users following routing recommendations provided by a navigation system, η can be modified by deciding the frequency at which travel recommendations are updated. For this reason, in what follows, we refer to η to as *imitation rate.* We illustrate the interconnection (13) and the quantities that establish the coupling between the two models in Fig. 3.

We next introduce some basic notation that will be used in the remainder. Since (12) ensures conservation of flows at the nodes, it guarantees that the vector of link flows y^l is an equilibrium for (4), namely,

$$0 = (R(y)^\mathsf{T} - I)y^l + R_o(y)\lambda. \tag{14}$$

From (14), we deduce that a set of demanded path flows y implicitly defines a set of *demanded densities* corresponding to these flows. These are defined as:

$$\varphi(y) := f^{-1}(y^l), \text{ where } y_i^l = \sum_{p\in\mathcal{P}:i\in p} y_p, \ \forall i \in \mathcal{L},$$

and $f^{-1} : \mathbb{R}^n_{\geq 0} \to \mathbb{R}^n_{\geq 0}$ denotes the entrywise inverse function of $f(\cdot)$. In words, the function $\varphi(y)$ maps a vector of demanded flows into the corresponding (demanded) densities. Similarly to demanded flows, demanded densities are virtual densities, which may never be observed in the network, and that model the amount of traffic density needed to support the instantaneous demanded flows $y(t)$.

We conclude this section by stressing that the flows on the links $f(x(t))$ imposed by the traffic dynamics differ from the demanded flows $y^l(t)$, which are imposed by the path selection model. We discuss in Remark 2.7 the important differences between these two quantities.

*Remark 2.7 (**Demanded flows vs actual flows**)*: It is important to stress a conceptual difference between "demanded" traffic variables and traffic variables imposed by the traffic dynamics. Regarding traffic flows, the vector of *traffic flows* $f(x(t))$ describes the flows on the links imposed by the traffic dynamics; on the other hand, the vector of *demanded traffic flows* $y^l(t)$ describes the fraction of flow demand λ entering at o and that is routed to the links based on an economic process of path selection. Analogously, the *traffic densities* $x(t)$ are quantities that are imposed by the physics, while the *demanded traffic densities* $\varphi(y)$ are virtual quantities describing the densities associated with the the traffic demand. Importantly, the *traffic latencies* $\ell(x)$ describe the actual travel latencies imposed by the physics, which in general differ from the *demanded traffic latencies* $\ell(\varphi(y))$. Notice that the two quantities converge to each other as the dynamics of the traffic physics become infinitely fast. This discrepancy differentiates our framework from the classical routing game [5], where the dynamics of traffic are infinitely fast. □

D. Connections with game-theoretic framework

In this section, we show that our framework can be related to a population game [33]. This will allows us to connect our setting to the routing game [9] and to relate the equilibirum points of the model (13) to Wardrop equilibria [25].

The replicator equation (9) naturally defines an associated population game [33], as described next. A (cost-minimization) population game is defined by the triple $(\mathcal{S}, \mathcal{X}, \kappa)$, where $\mathcal{S}$ is a set of pure strategies, $\mathcal{X}$ is a (generalized) simplex, and $\kappa : \mathcal{X} \to \mathbb{R}^{|\mathcal{S}|}$ is a vector-valued cost function describing the cost associated with each strategy, see [33, Sec. 13.2]. The replicator equation (9) implicitly defines a population game defined by

$$\mathcal{S} = \mathcal{P}, \qquad \mathcal{X} = \Delta', \qquad \kappa(y) = \ell \circ \varphi(y), \tag{15}$$

which in what follows we denote by $\mathcal{R}_{\Delta'} := (\mathcal{P}, \Delta', \ell \circ \varphi)$. In line with the existing literature [33], we will call a vector of the simplex $y \in \Delta'$ a (mixed) *strategy*. To this end, we will say that a strategy $y_{\text{br}} \in \Delta'$ is a *best reply* to y if:

$$y_{\text{br}}^\mathsf{T}\, \ell(\varphi(y)) \leq w^\mathsf{T} \ell(\varphi(y)), \qquad \forall w \in \Delta'.$$

Associated with $\mathcal{R}$, we have the following classical notion.

*Definition 2.8 (**Nash Equilibrium**)*: A vector $y^* \in \Delta'$ is said to be a *Nash equilibrium* of $\mathcal{R}_{\Delta'}$ if

$$\langle y^*, \ell(\varphi(y^*))\rangle \leq \langle y, \ell(\varphi(y^*))\rangle, \qquad \forall y \in \Delta'. \tag{16}$$

□

In other words, a Nash equilibrium is a best reply to itself. By noting that $y^\mathsf{T}\ell(\varphi(y))$ is the average population latency or cost (cf. (10)), a Nash equilibrium describes a situation where the population has no incentive to deviate away from strategy y as any other strategy will yield a non-smaller latency. Nash equilibria are used to describe routing games governed by selfish individuals, where each individual chooses their path to minimize their travel cost.

A very useful reformulation of the notion of Nash equilibrium is that of Wardrop equilibrium [34]: y is a Wardrop equilibrium if, for all $p \in \mathcal{P}$,

$$y_p > 0 \text{ implies } \ell_p(\varphi(y)) \leq \ell_{p'}(\varphi(y)), \ \forall p' \in \mathcal{P}. \tag{17}$$

In line with the findings of [34], in what follows we will use the wording Nash equilibrium and Wardrop equilibrium interchangeably.

A desirable property for Nash equilibria is that of *evolutionary stability*. Intuitively, a strategy $y \in \Delta'$ is evolutionary stable if it is a Nash equilibrium and small perturbations from this strategy have a strictly larger average latency.

*Definition 2.9 (**Evolutionary stable point**)*: A vector $y \in \Delta'$ is said to be an *evolutionary stable point* of $\mathcal{R}_{\Delta'}$ if it is a Nash equilibrium and, for all $w \in \Delta', w \neq y$,

$$w^\mathsf{T}\ell(\varphi(y)) = y^\mathsf{T}\ell(\varphi(y)) \text{ implies } w^\mathsf{T}\ell(w) > y^\mathsf{T}\ell(\varphi(w)). \tag{18}$$

□

In words, y is evolutionary stable if any other best response w to y is not a Nash equilibrium. It is worth stressing that evolutionary stability is a property of the game $\mathcal{R}$ as it is defined independently of the choice of the vector field in (9).

We conclude this section with an important observation, which highlights the novelty of the model in Section II with respect to the classical routing game framework [9]. We remark that, in the routing game, both the traffic and path selection mechanisms operate at the Nash equilibrium [9] at all times. This requirement implicitly makes two highly limiting assumptions: (i) the highways have trivial (infinitely fast) dynamics so that the traffic flows can be modeled as an algebraic map $\varphi(y)$ of the flow demands; (ii) there are no transients in the path selection process, so that the path preferences can be described as a Nash equilibrium (16) at all times. Remarkably, when the framework of the routing game framework was derived in the 1950s [9], travelers could update their routing preferences only from day to day and networks would often operate near equilibrium as traffic demands would change slowly. In contrast, in modern networks, travelers can update their routing preferences at a fast timescale, as they have access to instantaneous real-time traffic information, and traffic demands are highly dynamic. Hence, we conjecture that the model proposed here is a more accurate description of modern traffic systems.

III. Properties of the Equilibrium Points

In this section, we study the properties of the equilibrium points of the interconnection (13). We begin by noting that solutions to (13) are well-defined, as formalized next.

*Proposition 3.1 (**Well-posedness of solutions**)*: Let Assumptions 1 and 2 be satisfied, $x(0) \in \mathbb{R}^n_{\geq 0}$, and $y(0) \in \Delta'$. Then, there exists a unique solution

$(x(t), y(t)), t \geq 0$, to the initial value problem (13). Moreover, $(x(t), y(t)) \in \mathbb{R}^n_{\geq 0} \times \Delta'$ for all $t \geq 0$. □

Proof: Existence and uniqueness of the solutions follow from the Lipschitz continuity of the vector fields in (13). The claim $x(t) \in \mathbb{R}^n_{\geq 0}$ follows from Assumption 1, and $y(t) \in \Delta'$ follows from $\sum_{p\in\mathcal{P}} \dot{y}_p = 0$. ■

A. Existence of fixed points

We begin by investigating under what conditions the interconnected model (13) admits equilibrium points. Interestingly, we will show that their existence depends solely on the magnitude of external inflows entering the network. To this end, the min-cut capacity of the traffic flow model is:

$$C_{\text{cut}} = \min_{\substack{\mathcal{S}\subseteq\mathcal{V}:\\ o\in\mathcal{S}, d\notin\mathcal{S}}} \sum_{\substack{i\in\mathcal{L}:\\ o_i\in\mathcal{S}, d_i\notin\mathcal{S}}} C_i.$$

Notice that C_{cut} may or may not be finite, precisely, $C_{\text{cut}} \in [0, +\infty]$.

*Proposition 3.2 (**Existence of equilibria**):* Let Assumptions 1 and 2 be satisfied. If $\lambda < C_{\text{cut}}$, then the interconnected system (13) admits an equilibrium point that is a Nash equilibrium. Conversely, if $\lambda > C_{\text{cut}}$, then, no equilibirum point exists for (13). □

Proof: (Case $\lambda < C_{\text{cut}}$) To prove this implication, we show the existence of a point that satisfies the Wardrop conditions and that is an equilibrium of (13). Following [5, Thm. 2.1], a vector of path flows $\bar{y} \in \mathbb{R}^{|\mathcal{P}|}$ is a Wardrop equilibrium if and only if it satisfies the first-order optimality conditions of the following optimization problem:

$$\min_{y_1,\dots,y_{|\mathcal{P}|}\in\mathbb{R}} \quad \sum_{i\in\mathcal{L}} \int_0^{y_i^l} \ell_i^l(s)ds, \tag{19a}$$

$$\text{s. to} \quad \sum_{p\in\mathcal{P}} y_p = \lambda, \tag{19b}$$

$$y_p \geq 0, \ \forall p \in \mathcal{P}, \tag{19c}$$

$$\sum_{p\in\mathcal{P}: i\in\mathcal{P}} y_p = y_i^l, \ \forall i \in \mathcal{L}, \tag{19d}$$

In (19), $y_1^l, \dots, y_n^l$ are dependent variables (describing link flows) that are uniquely determined by (19d) (see [5, Thm 2.2]). Since the objective function is continuous and non-decreasing (cf. Assumption 2), according to Weierstrass' Theorem, it admits a minimum provided that the feasible set is closed, bounded, and nonempty. The feasible set of (19) is unbounded, but from the positiveness of the latency functions, one may add the constraint $y_p \leq d_p$, where $d_p > 0$ is sufficiently large. Hence, the feasible set can be made closed and bounded without affecting the solution of [5, Thm 2.1]. Since $\lambda < C_{\text{cut}}$, by the max-flow min-cut theorem [35, Thm 4.1], the feasible set is nonempty. Hence, by Weierstrass' Theorem, the game $\mathcal{R}$ admits a Nash equilibrium.

Let y^* denote a Nash equilibrium of $\mathcal{R}$; we next show that y^* is an equilibrium flow for (13a). Let $R(y^*)$ be the routing matrix obtained from y^* via (12); by using (14), we have

$$(R(y^*)^\mathsf{T} - I)\varphi(y^*) + \lambda = 0,$$

and thus we conclude that the pair $(x^*, y^*), x^* := \varphi(y^*)$, is an equilibrium of (13a). We are left to show that (x^*, y^*), is also an equilibrium of (13b). Since y^* is a Nash equilibrium, it satisfies:

$$\ell_p(\varphi(y^*)) = c, \qquad \forall p \in \mathcal{P} : \bar{y}_p > 0,$$

and thus we have $\bar{\ell}(\varphi(y^*), y^*) = c$. This proves that (x^*, y^*), is an equilibrium of (13b).

(Case $\lambda > C_{\text{cut}}$) By contradiction, assume that an equilibrium point (x^*, y^*) exists. Because the replicator equation guarantees $y(t) \in \Delta'$ $\forall t \geq 0$, we must have

$$\sum_{p\in\mathcal{P}} y_p^* = \lambda \text{ and } y_p^* \geq 0, \qquad \forall p \in \mathcal{P}.$$

Under these two conditions, the max-flow min-cut theorem is applicable, which guarantees that, for some $i \in \mathcal{L}$,

$$\sum_{p\in\mathcal{P}: i\in\mathcal{P}} y_p^* > C_i, \tag{20}$$

but this contradicts the equilibrium condition $(R(y^*)^\mathsf{T} - I)\varphi(y^*) + \lambda = 0$, thus proving the claim. ■

In words, fixed points exist when the external flow demand is bounded above by the min-cut capacity; moreover, at least one equilibrium point is a Wardrop equilibrium. This has two important implications. First, it shows that our model is consistent with the classical literature, in particular, with the widely established notion of Wardrop equilibrium. Importantly, while Wardrop equilibria were developed for static models operating at equilibrium, our model instead is a dynamic generalization of this classical framework [5]. Second, the result relates our work with the fundamental bound concerning the maximum amount of flow transferable by a static graph (as given by the max-flow min-cut theorem [35]): it shows that traffic systems where users learn through imitation can transfer, asymptotically, the same amount of flow as static graphs with free routing. This implies that imitation-based selection benefits the overall traffic system, enabling it to transfer the maximum admissible amount of flow. We remark that this property is in contrast with dynamic traffic flow models with static routing, which may not admit equilibrium points even when $\lambda < C_{\text{cut}}$ (see, e.g., [6], [16, Prop. 2]).

B. Conditions for uniqueness of the Nash equilibrium

While Proposition 3.2 guarantees existence of a Nash equilibrium, it remains unclear whether such an equilibrium is unique or evolutionary stable. We address this aspect next.

*Proposition 3.3 (**Uniqueness and evolutionary stability**):* Let Assumptions 1–2 be satisfied and $\mathcal{R}_{\Delta'}$ be the game induced by (9) and defined as in (15). Further, assume that the latency functions are strictly monotone, namely, for all $i \in \mathcal{L}$,

$$(x_i - \bar{x}_i)(\ell_i^l(x_i) - \ell_i^l(\bar{x}_i)) > 0, \tag{21}$$

for all $x_i, \bar{x}_i \in [0, C_i), x_i \neq \bar{x}_i$. Then, the game $\mathcal{R}_{\Delta'}$ admits a unique Nash equilibrium. Moreover, such equilibrium is evolutionary stable.

The following lemma is instrumental for the proof.

*Lemma 3.4 (**Strict monotonicity of the flow latencies**):* Under the assumptions of Proposition 3.3, the demanded path flow latency functions are strictly monotone, namely,

$$\langle y-\bar{y}, \ell(\varphi(y))-\ell(\varphi((\bar{y}))\rangle > 0, \quad \forall y,\bar{y}\in\Delta', y\neq\bar{y}. \tag{22}$$

□

Proof: We have:

$$\begin{aligned}
&\langle y-\bar{y}, \ell(\varphi(y))-\ell(\varphi((\bar{y}))\rangle \\
&\quad= \sum_{p\in\mathcal{P}}(y_p-\bar{y}_p)(\ell_p(\varphi(y))-\ell_p(\varphi(\bar{y}))) \\
&\quad= \sum_{p\in\mathcal{P}}(y_p-\bar{y}_p)\left(\sum_{i\in p}\ell_i^l(\varphi_i(y))-\sum_{i\in p}\ell_i^l(\varphi_i(\bar{y}))\right) \\
&\quad= \sum_{i\in\mathcal{L}}\sum_{p\in\mathcal{P}:i\in p}(y_p-\bar{y}_p)\left(\ell_i^l(\varphi_i(y))-\ell_i^l(\varphi_i(\bar{y}))\right) \\
&\quad= \sum_{i\in\mathcal{L}}(y_i^l-\bar{y}_i^l)\left(\ell_i^l(\varphi_i(y))-\ell_i^l(\varphi_i(\bar{y}))\right),
\end{aligned}$$

where the second identity follows from (7) and the fourth identity from (6). Next, let $i\in\mathcal{L}$ be fixed, and distinguish among three cases. (Case 1) Assume $y_i^l>\bar{y}_i^l$, we have:

$$(y_i^l-\bar{y}_i^l)\left(\ell_i^l(\varphi_i(y))-\ell_i^l(\varphi_i(\bar{y}))\right)>0, \tag{23}$$

since ϕ_i and ℓ_i^l are strictly increasing. (Case 2) Assume $y_i^l<\bar{y}_i^l$. In this case, (23) also holds since φ_i and ℓ_i^l are strictly increasing. (Case 3) Assume $y_i^l=\bar{y}_i^l$. We have:

$$(y_i^l-\bar{y}_i^l)\left(\ell_i^l(\varphi_i(y))-\ell_i^l(\varphi_i(\bar{y}))\right)=0.$$

Since $y\neq\bar{y}$, there exists at least one link $i\in\mathcal{L}$ for which (23) is satisfied, from which we conclude that (22) holds. ■

We are now ready to prove the proposition

Proof of Proposition 3.3: Let $y^*\in\Delta'$ denote a Nash equilibrium of $\mathcal{R}_{\Delta'}$ and $y\in\Delta'$. Using (16), we have

$$\langle y^*,\ell(\varphi(y^*))\rangle+\langle y,\ell(\varphi(y))\rangle\leq\langle y,\ell(\varphi(y^*))\rangle+\langle y,\ell(\varphi(y))\rangle,$$

by re-arranging:

$$\begin{aligned}
\langle y,\ell(\varphi(y))\rangle &\geq \langle y^*,\ell(\varphi(y^*))\rangle+\langle y,\ell(\varphi(y))-\ell(\varphi(y^*)\rangle \\
&> \langle y^*,\ell(\varphi(y^*))\rangle+\langle y^*,\ell(\varphi(y))-\ell(\varphi(y^*)\rangle \\
&= \langle y^*,\ell(\varphi(y))\rangle,
\end{aligned} \tag{24}$$

where the second row follows from (22) and the third row follows from re-arranging the terms. Inequality (24) proves (18), thus showing that y^* is evolutionary stable. Finally, since the above condition holds for all $y\in\Delta'$, no other point in Δ' other than y^* can satisfy (16), thus proving uniqueness. ■

Proposition 3.3 shows that, under an additional monotonicity requirement on the latency functions, the game $\mathcal{R}_{\Delta'}$ admits a unique Nash equilibrium that is evolutionary stable. See Fig. 4. We stress that uniqueness and evolutionary stability are properties of the Nash equilibrium of the game $\mathcal{R}_{\Delta'}$,

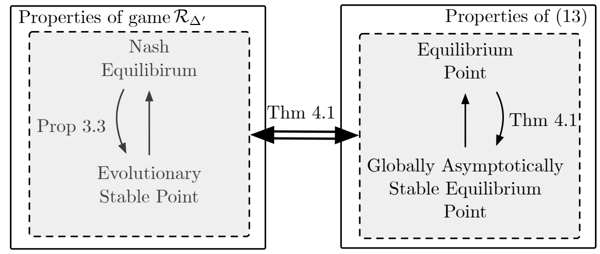

Fig. 4: Summary of the properties established in the main results of this paper. Proposition 3.3 shows existence of a unique Nash equilibirum and that such equilibirum is evolutionary stable; Theorem 4.1 shows that the unique Nash equilibrium of $\mathcal{R}_{\Delta'}$ is also an equilibrium point of (13) and that such a point is globally asymptotically stable.

(and not of the joint dynamics (13)). However, we will show in the next section that these properties can be harnessed to study the asymptotic properties of the trajectories of (13).

IV. Asymptotic stability of the Nash equilibrium

In this section, we study the stability properties of the equilibrium points of the interconnection (13). To proceed, we reinforce Assumption 2 as follows.

Assumption 3: The conditions in Assumption 2 are satisfied. Moreover, the latency functions are strongly monotone, namely, there exists $\sigma>0$ such that

$$(x_i-\bar{x}_i)(\ell_i^l(x_i)-\ell_i^l(\bar{x}_i))\geq\sigma|x_i-\bar{x}_i|^2, \tag{25}$$

for all $x_i,x_i'\in[0,C_i)$ and $i\in\mathcal{L}$. □

In words, the assumption asks that the latency functions grow at least linearly with the traffic densities[1]; the parameter σ quantifies the "steepness" of the density-latency maps. In what follows, we will interpret σ as a free parameter, which can be tuned by a system planner to improve the efficiency of a traffic system modeled by (13). The following result characterizes the asymptotic behavior of (13).

*Theorem 4.1 (**Stability of interconnected system**):* Let Assumption 1 and 3 hold and $\lambda<C_{\text{cut}}$. Let $(x(t),y(t))$ denote the solution of (13) with initial conditions $(x(0),y(0))$, Δ' the restricted simplex induced by $y(0)$, $\mathcal{R}_{\Delta'}$ the game defined by (15), and y^* the unique Nash equilibrium of $\mathcal{R}_{\Delta'}$. There exists $\sigma^*,\eta_1,\eta_2>0$ such that if σ and η satisfy:

$$\sigma>\sigma^*, \qquad \eta\in[\eta_1,\eta_2], \tag{26}$$

then, for any $(x(0),y(0))\in\mathbb{R}^n_{\geq0}\times\Delta'$,

$$\lim_{t\to\infty}\|(x(t),y(t))-(x^*,y^*)\|=0,$$

where $x^*:=\varphi(y^*)$. □

The following lemma is a minor extension of Lemma 3.4 under Assumption 3, and is instrumental for the proof.

*Lemma 4.2 (**Strong monotonicity of the flow latencies**):* When Assumptions 1 and 3 hold, the path flow latency

[1] Indeed, strong monotonicity of $\ell_i^l(x_i)$ is equivalent to imposing that $\ell_i^l(x_i)-\sigma x_i$ is a monotone function (this follows by rewriting the inequality as $(x_i-\bar{x}_i)((\ell_i^l(x_i)-\sigma x_i)-(\ell_i^l(\bar{x}_i)-\sigma x_i))\geq0$).

functions are strongly monotone, namely, there exists $\sigma > 0$:

$$\langle y - \bar{y}, \ell(\varphi(y)) - \ell(\varphi((\bar{y}))\rangle \geq \sigma\|y - \bar{y}\|^2, \quad \forall y, \bar{y} \in \Delta'. \tag{27}$$

□

Proof of Theorem 4.1: Our proof technique relies on showing that the potential function

$$V(x, y) := V_x(x) + V_y(y),$$

where $V_x(x)$ is a potential function for (13a) and $V_x(x)$ is a potential function for (13b) strongly decreases along the trajectories of (13) and achieves its minimum at $(\varphi(y^*), y^*)$. We will use the following compact notation:

$$A(y) := R(y)^\mathsf{T} - I, \qquad \phi(y) := -A(y)^{-1}R_o(y)\lambda,$$

with $\phi(y) = (\phi_1(y), \ldots, \phi_n(y))$. Since $\mathcal{G}$ is outflow connected, [36, Thm. 3] guarantees that $A(y)$ is invertible for any y. Since $-A(y^*)$ is a nonsingular M-matrix, [37, Prop. I_{25}] guarantees the existence of a positive diagonal matrix $D = \mathrm{diag}(d_1, \ldots, d_n)$ such that

$$Q = -(A(y^*)D + DA(y^*)), \tag{28}$$

is symmetric and positive definite. Let

$$V_x(x) := 2\sum_{i\in\mathcal{L}} d_i^{-1}\int_0^{x_i} f(s) - \phi_i(y^*)ds. \tag{29}$$

The time-derivative of $V_x(x)$ along the solutions of (13) is:

$$\begin{aligned}
\dot{V}(x) &= 2(f(x) - \phi(y^*))D^{-1}(A(y)f(x) + R_o(y)\lambda) \\
&= 2(f(x) - \phi(y^*))^\mathsf{T}D^{-1}(A(y^*)f(x) + R_o(y^*)\lambda) \\
&\quad + 2(f(x) - \phi(y^*))^\mathsf{T}D^{-1}(\psi_x(y) - \psi_x(y^*)) \\
&= -(f(x) - \phi(y^*))^\mathsf{T}Q(f(x) - \phi(y^*)) \\
&\quad + 2(f(x) - \phi(y^*))^\mathsf{T}D^{-1}(\psi_x(y) - \psi_x(y^*)) \\
&\leq -\mu\lambda_{\min}(Q)\|x - \varphi(y^*)\|^2 + k\|x - \varphi(y^*)\|\|y - y^*\| \\
&\leq -\frac{\mu\lambda_{\min}(Q)}{2}\|x - \varphi(y^*)\|^2 + \frac{k^2}{2\mu\lambda_{\min}(Q)}\|y - y^*\|^2.
\end{aligned} \tag{30}$$

Here, in the second row, we used the compact notation

$$\psi_x(y) := A(y)f(x) + R_o(y)\lambda,$$

the third row follows from (28). The fourth row follows by using the Cauchy-Schwarz inequality and by noting that $\psi_x(y)$ is Lipschitz continuous in y, uniformly in x, and by letting $k = 2\|D^{-1}\|L_\psi L_f$, where L_ψ and L_f denote the Lipschitz constants of $\psi_x(\cdot)$ and $f(\cdot)$, respectively. The fifth row follows from the inequality $-ax^2 + bx \leq b^2/4a$ for $a, b > 0, x \in \mathbb{R}$.

Next, we let

$$V_y(y) = \sum_{p\in\mathcal{P}} y_p^* \ln\left(\frac{y_p^*}{y_p}\right).$$

The time-derivative of $V_y(y)$ along the solutions of (13) is given by:

$$\begin{aligned}
\dot{V}_y(y) &= -\eta\sum_p y_p^*(\bar{\ell}(x, y) - \ell_p(x)) \\
&= -\lambda\bar{\ell}(x, y) + \eta\sum_p y_p^*\ell_p(x) \\
&= -\eta\sum_p(y_p - y_p^*)\ell_p(x) \\
&= -\eta\sum_p(y_p - y_p^*)\ell_p(\varphi(y)) \\
&\quad - \eta\sum_p(y_p - y_p^*)(\ell_p(x) - \ell_p(\varphi(y)) \\
&\leq -\eta\sigma\|y - y^*\|^2 + \eta L_\ell\|y - y^*\|\|x - \varphi(y)\|
\end{aligned} \tag{31}$$

Here, the second row follows from $\sum_p y_p^* = \lambda$; the third row follows from (10); the fourth row from adding and subtracting $\ell_p(\varphi(y))$. The fifth row follows by application of the Cauchy-Schwarz inequality, by using continuity of $\ell(\cdot)$ (where L_ℓ denotes the corresponding Lipschitz constant), and from the following inequality:

$$\langle y - y^*, \ell(\varphi(y))\rangle \geq \sigma\|y - y^*\|^2. \tag{32}$$

To prove (32), since y^* is a Nash equilibrium, we have from (16):

$$\langle y^*, \ell(\varphi(y^*))\rangle + \langle y, \ell(\varphi(y))\rangle \leq \langle y, \ell(\varphi(y^*))\rangle + \langle y, \ell(\varphi(y))\rangle,$$

by re-arranging:

$$\begin{aligned}
&\langle y, \ell(\varphi(y))\rangle \geq \langle y^*, \ell(\varphi(y^*))\rangle + \langle y, \ell(\varphi(y)) - \ell(\varphi(y^*)\rangle \\
&\quad > \langle y^*, \ell(\varphi(y^*))\rangle + c\|y - y^*\|^2 + \langle y^*, \ell(\varphi(y)) - \ell(\varphi(y^*)\rangle \\
&\quad = \langle y^*, \ell(\varphi(y))\rangle + c\|y - y^*\|^2,
\end{aligned} \tag{33}$$

where the second row follows from Lemma 4.2. This proves (32). We can further bound (31) as:

$$\begin{aligned}
\dot{V}_y(y) &\leq -\eta(\sigma - L_\ell L_\varphi)\|y - y^*\|^2 \\
&\qquad + \eta L_\ell\|y - y^*\|\|x - \varphi(y^*)\| \\
&\leq -\eta(\frac{\sigma}{2} - L_\ell L_\varphi)\|y - y^*\|^2 + \frac{\eta L_\ell^2}{2\sigma}\|x - \varphi(y^*)\|^2,
\end{aligned} \tag{34}$$

where the first inequality follows from the Cauchy-Schwarz inequality and by continuity of $\varphi(\cdot)$ (where L_φ denotes the corresponding Lipschitz constant), and the second row follows from the inequality $-ax^2 + bx \leq b^2/4a$ for $a, b > 0, x \in \mathbb{R}$.

By combining (30) and (34) we conclude:

$$\dot{V}(x, y) \leq -c_1\|x - \varphi(y^*)\|^2 - c_2\|y - y^*\|^2, \tag{35}$$

where the constants c_1 and c_2 are given by:

$$c_1 := \frac{\mu\lambda_{\min}(Q)}{2} - \frac{\eta L_\ell^2}{2\sigma}, \quad c_2 := \eta\left(\frac{\sigma}{2} - L_\ell L_\varphi\right) - \frac{k^2}{2\mu\lambda_{\min}(Q)}.$$

We thus have that $c_1 \geq 0$ and $c_2 \geq 0$ when, respectively,

$$\eta \leq \eta_2 := \frac{\mu\sigma\lambda_{\min}(Q)}{L_\ell^2}, \quad \eta \geq \eta_1 := \frac{k^2}{\mu\lambda_{\min}(Q)(\sigma - L_\ell L_\varphi)}. \tag{36}$$

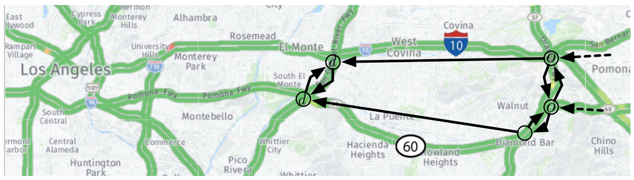

(a)

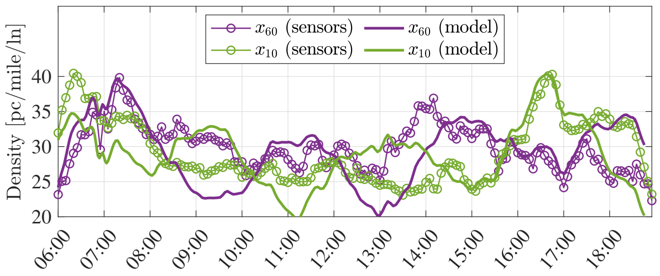

(b)

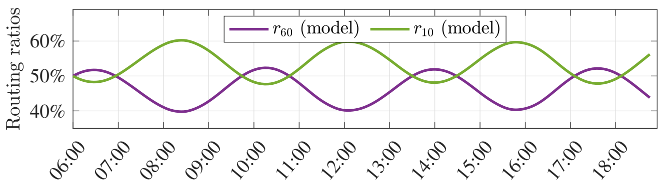

(c)

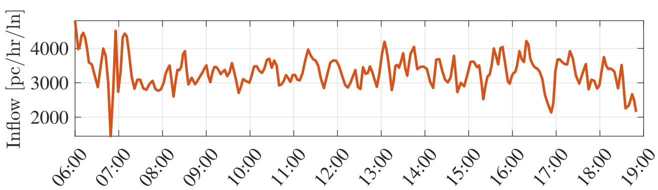

(d)

Fig. 5: Time series data for SR60-W and I10-W on March 6, 2020. Results obtained by identifying the parameters of (13) using a prediction-correction algorithm that minimizes the fitting error. (a) Traffic network and graph. (b) Traffic flow data obtained from sensors (continuous lines with circles) and traffic state predicted by our models (continuous lines). (c) Routing predicted by our models. (d) Combined traffic demand entering at the origin. The data illustrates a case where the trajectories of (13) oscillate and thus the equilibria lack to be asymptotically stable.

Thus, there exists a feasible choice of η that guarantees that $c_1 \geq 0$ and $c_2 \geq 0$ when $\sigma > \sigma_1 := 2L_\ell L_\varphi$ and

$$\frac{k^2}{\mu\lambda_{\min}(Q)(\sigma - L_\ell L_\varphi)} \leq \frac{\mu\sigma\lambda_{\min}(Q)}{L_\ell^2}. \tag{37}$$

Notice that (37) can always be guaranteed to hold, provided that σ is chosen sufficiently large. Altogether this implies that when $\sigma > \sigma^*$ – where $\sigma^* = \max\{\sigma_1, \sigma_2\}$ and σ_2 is the smallest value of σ such that (37) holds – and $\eta \in [\eta_1, \eta_2]$, $V(x, y)$ decreases towards its minimum, given by $\xi(x, y) = 0$, which implies $(x, y) = (\varphi(y^*), y^*)$. The claim thus follows by application of La Salle's invariance principle [38, Cor. 4.1]. ■

We illustrate in Fig. 4 the relationships between implications. The theorem shows that, provided that the latency functions are sufficiently steep and the imitation rate η is adequately chosen (as in (26)), the trajectories of (13) converge to the unique Nash equilibrium of the game $\mathcal{R}_{\Delta'}$ from any initial condition. We note that, although the statement provides an existence result for σ^*, η_1, η_2, an explicit expression for these quantities is given in the proof in (36) and (37). Intuitively, (37) states that as σ increases, the interval $[\eta_1, \eta_2]$ becomes wider since $\eta_1 \to 0$ and $\eta_2 \to +\infty$. In words, this implies that the steeper the latency functions, the more freedom one has in the choice of η.

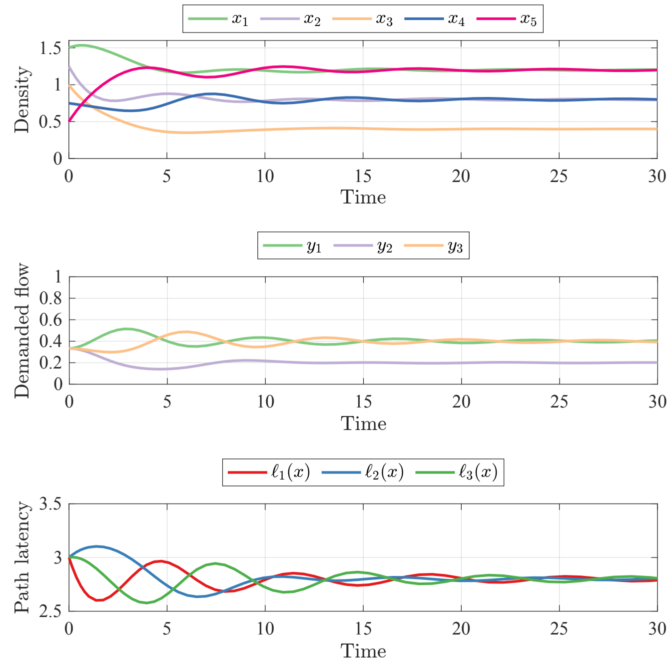

Fig. 6: Time evolution of the state trajectories of the model (13) for the network in Fig. 1 with the choice $\eta = 1$. (Top) Evolution of the traffic density state x. (Middle) Evolution of the demanded path flow state. (Bottom) Evolution of the travel latencies on the paths. The choice $\eta = 1$ belongs to the range of stabilizing values characterized in Theorem 4.1, and thus guarantees that the state asymptotically converges to the Nash equilibrium of the underlying game.

Interestingly, the result suggests that asymptotic stability may fail to hold when the latency functions are not sufficiently steep, or the imitation rate is either too small or too large. Intuitively, when σ is small, the path selection process is not sufficiently sensitive to variations of traffic congestion on the links. On the other hand, when η is too large, the population is overreacting to small changes in congestion, and individual users update their preferences without anticipating the strategy of the rest of the population.

V. Simulation Results

This section presents two sets of numerical simulations that illustrate our findings.

A. Study case from California SR60-W and I10-W

Consider the traffic network in Fig. 5(a), which schematizes the west bounds of the freeways SR60-W and I10-W in Southern California. Let x_{60} and x_{10} be the average traffic density in the examined sections of SR60-W (absolute miles $13.1 - 22.4$) and in the section of I10-W (absolute miles $24.4 - 36.02$), respectively. Moreover, let r_{60} (resp. $r_{10} =$

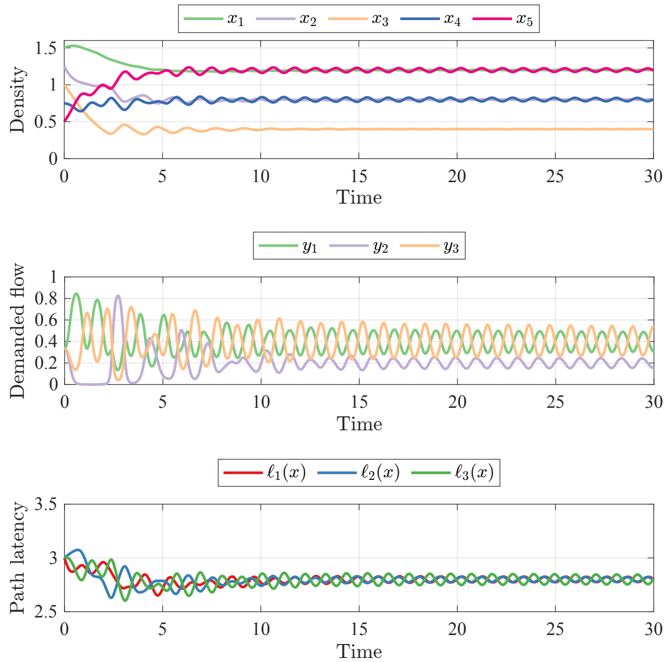

Fig. 7: Time evolution of the state trajectories of the model (13) for the network in Fig. 1 with the choice $\eta = 1$. (Top) Evolution of the traffic density state x. (Middle) Evolution of the demanded path flow state. (Bottom) Evolution of the travel latencies on the paths. The choice $\eta = 30$ does not belong to the range of stabilizing values characterized in Theorem 4.1. As illustrated in the simulations, this choice of η originates oscillating trajectories, describing a condition where users repeatedly switch their path preferences.

$1 - r_{60}$) be the fraction of travelers choosing freeway SR60-W over I10-W (resp. choosing freeway I10-W over SR60-W) for their commute. Fig. 5(b) illustrates the time-evolution of the recorded traffic densities on the two highways on Friday, March 6, 2020, reconstructed using data from the *Caltrans Freeway Performance Measurement System (PeMS)*; in the same figure, we show the time-evolution of the state of the interconnected model (13). The parameters of the traffic system (4) were derived from the nominal highway characteristics provided by the PeMS. For the routing model (9), the link latency functions are computed by integrating traffic speed data. This data illustrates a case where the trajectories of (13) oscillate over time, implying that the equilibrium points lack to be asymptotically stable; this showcases a scenario where the assumptions of Theorem 4.1 are not satisfied in practice.

B. Illustrative simulations on synthetic model

Consider the network illustrated in Fig. 1 and discussed in Examples 2.4-2.6. Consider a model where $\lambda = 1$, for all $i \in \mathcal{L}$ the outflow functions are linear $f_i(x_i) = 0.5x_i$, and the latency functions are given by $\ell_i(x_i) = x_i, i \in \{1, 3, 5\}$ and $\ell_i(x_i) = 2x_i, i \in \{2, 4\}$. Notice that these choices satisfy Assumption 1 and 3. Proposition 3.2 guarantees that the game $\mathcal{R}_{\Delta'}$ admits an equilibrium point; by Proposition 3.1 such equilibrium is unique and evolutionary stable. Solving (19), one obtains the Nash equilibrium $y^* = (2/5, 1/5, 2/5)$. It is then possible to use Theorem 4.1 to determine values of η that guarantee that the trajectories of (13) converge to the Nash equilibrium. For our choices of functions, one can verify by inspection that $\mu = 0.5, L_f = 0.5, \sigma = 1, L_\ell = 2, \sigma = 1$. Moreover, we estimated numerically (sampling each variable uniformly in their domain using a Latin Hypercube technique) $L_\varphi = 0.125, L_\psi = 1.1547$. We used $D = 10^2 I$ and obtained matrix Q (cf. (28)) with $\lambda_{\min}(Q) = 20$. This yields $k = 0.2039$. With these choices, it is easy to see that (37) is verified, and $\eta_1 = 2.6667\ 10^{-6}, \eta_2 = 25$. Fig. 6 illustrates the state trajectories of (13) for $\eta = 1$. As anticipated by Theorem 4.1, the state trajectories converge to the Nash equilibrium of the game $\mathcal{R}_{\Delta'}$. On the other hand, Fig. 7 illustrates the state trajectories of the interconnected system with the choice $\eta = 30$. The simulation demonstrates that an inadequate choice of imitation rate η leads to trajectories that oscillate over time and not approach the Nash equilibrium. The drawbacks of this oscillating phenomenon can be visualized by comparing the path latencies illustrated in the bottom figures of Fig. 6 and Fig. 7. The choice $\eta = 1$ guarantees that all used paths have the same latency at equilibrium, thus ensuring that all users experience the same travel time. On the other hand, with the choice $\eta = 50$, travel latencies are not homogeneous across the three paths, implying that certain users experience a worse travel time and higher congestion. From our simulations, we observed that the amplitude of oscillating trajectories increases with the flow demand λ, thus suggesting that the suboptimality discussed above could deteriorate with increased congestion.

VI. Conclusions

This paper proposed a dynamic model of traffic and path selection to describe the impact of app-informed travelers in modern traffic networks. We studied the properties and stability of the equilibrium points of this model, showing that it is consistent with existing studies in transportation. Our results suggest that the general adoption of navigation systems enables these networks to transfer an amount of flow no smaller than the min-cut capacity, and that the equilibrium points are asymptotically stable provided that the latency functions are sufficiently sensitive and the imitation rate is adequately chosen. Future studies should investigate how our conclusions translate to more general models that account for bounded supply back propagation through the junctions. Our results give rise to several opportunities for future work. By coupling these models with common infrastructure control models (such as variable speed limits and freeway metering), these results may play an important role in designing dynamic controllers for congested infrastructures. Furthermore, our models and stability analysis represents a fundamental framework for future studies on robustness and security analysis.

References

[1] M. Sprung, M. Chambers, and S. Smith-Pickel, “Transportation statistics annual report 2018,” U.S. Department of Transportation, Tech. Rep., 2018. [Online]. Available: https://rosap.ntl.bts.gov/view/dot/37861

[2] European Commission, “Clean transport, urban transport: Urban mobility,” https://ec.europa.eu/transport/themes/urban/urban_mobility_en, 2020, [Online; accessed 3-Jan-2020].

[3] J. C. Herrera, D. B. Work, R. Herring, X. J. Ban, Q. Jacobson, and A. M. Bayen, "Evaluation of traffic data obtained via GPS-enabled mobile phones: The mobile century field experiment," *Transp. Research Pt. C: Emerging Technologies*, vol. 18, no. 4, pp. 568–583, 2010. doi: 10.1016/j.trc.2009.10.006.

[4] A. Keimer, N. Laurent-Brouty, F. Farokhi, H. Signargout, V. Cvetkovic, A. M. Bayen, and K. H. Johansson, "Information patterns in the modeling and design of mobility management services," *Proceedings of the IEEE*, vol. 106, no. 4, pp. 554–576, 2018. doi: 10.1109/jproc.2018.2800001.

[5] M. Patriksson, *The traffic assignment problem: models and methods*. Mineola, NY: Dover Publications, 2015. ISBN 0486787907

[6] C. F. Daganzo, "The cell transmission model pt. II: network traffic," *Transp. Research Pt. B: Methodological*, vol. 29, no. 2, pp. 79–93, 1995. doi: 10.1016/0191-2615(94)00022-r.

[7] J. W. Weibull, *Evolutionary game theory*. MIT press, 1997. ISBN 0262731215

[8] T. Börgers and R. Sarin, "Learning through reinforcement and replicator dynamics," *Journal of Economic Theory*, vol. 77, no. 1, pp. 1 – 14, 1997. doi: 10.1006/jeth.1997.2319.

[9] T. Roughgarden, *Selfish routing and the price of anarchy*. MIT press, 2005. doi: doi.org/10.21236/ada637949.

[10] A. Bayen, A. Keimer, E. Porter, and M. Spinola, "Time-continuous instantaneous and past memory routing on traffic networks: A mathematical analysis on the basis of the link-delay model," *SIAM Journal on Applied Dynamical Systems*, vol. 18, no. 4, pp. 2143–2180, 2019. doi: doi.org/10.1137/19m1258980.

[11] A. Keimer and A. Bayen, "Routing on traffic networks incorporating past memory up to real-time information on the network state," *Annual Review of Control, Robotics, and Autonomous Systems*, vol. 3, pp. 151–172, 2020. doi: 10.1146/annurev-control-091319-125444.

[12] A. Festa and P. Goatin, "Modeling the impact of on-line navigation devices in traffic flows," in *IEEE Conf. on Decision and Control*, 2019. doi: 10.1109/cdc40024.2019.9030208. pp. 323–328.

[13] T. Jérôme, N. Laurent-Brouty, and A. M. Bayen, "Negative externalities of GPS-enabled routing applications: A game theoretical approach," in *IEEE Conf. on Intelligent Transportation Systems*, 2016. doi: 10.1109/itsc.2016.7795614. pp. 595–601.

[14] S. Fischer and B. Vöcking, "On the evolution of selfish routing," in *European Symposium on Algorithms*, 2004. doi: 10.1007/978-3-540-30140-0_30. pp. 323–334.

[15] W. Krichene, B. Drighès, and A. M. Bayen, "Online learning of nash equilibria in congestion games," *SIAM Journal on Control and Optimization*, vol. 53, no. 2, pp. 1056–1081, 2015. doi: 10.1137/140980685.

[16] S. Coogan and M. Arcak, "A compartmental model for traffic networks and its dynamical behavior," *IEEE Transactions on Automatic Control*, vol. 60, no. 10, pp. 2698–2703, 2015. doi: 10.1109/TAC.2015.2411916.

[17] G. Como, K. Savla, D. Acemoglu, M. A. Dahleh, and E. Frazzoli, "Stability analysis of transportation networks with multiscale driver decisions," *SIAM Journal on Control and Optimization*, vol. 51, no. 1, pp. 230–252, 2013. doi: 10.1109/acc.2011.5991560.

[18] S. Coogan and M. Arcak, "Stability of traffic flow networks with a polytree topology," *Automatica*, vol. 66, pp. 246–253, 2016. doi: 10.1016/j.automatica.2015.12.015.

[19] G. Bianchin and F. Pasqualetti, "Routing apps may cause oscillatory congestions in traffic networks," in *IEEE Conf. on Decision and Control*, Jeju Island, Republic of Korea, Dec. 2020. doi: 10.1109/CDC42340.2020.9303866. . ISSN 2576-2370 pp. 253–260.

[20] G. Como and R. Maggistro, "Distributed dynamic pricing of multiscale transportation networks," *IEEE Transactions on Automatic Control*, vol. 67, no. 4, pp. 1625–1638, 2021. doi: 10.1109/tac.2021.3065193.

[21] T. Toso, A. Y. Kibangou, and P. Frasca, "Impact on traffic of delayed information in navigation systems," *IEEE Control Systems Letters*, 2023. doi: 10.1109/lcsys.2023.3273170. Early access.

[22] ——, "Modeling the impact of route recommendations in road traffic," in *IFAC World Conference*, 2023, to appear.

[23] Y. Nie, "Equilibrium analysis of macroscopic traffic oscillations," *Transp. Research Pt. B: Methodological*, vol. 44, no. 1, pp. 62 – 72, 2010. doi: 10.1016/j.trb.2009.06.002.

[24] S. Chen, H. Yu, and M. Krstic, "Regulator design for a congested continuum traffic model with app-routing instability," in *2020 American Control Conference (ACC)*, 2020. doi: 10.23919/acc45564.2020.9147386. pp. 4515–4520.

[25] J. G. Wardrop, "Some theoretical aspects of road traffic research," *Proceedings of the institution of civil engineers*, vol. 1, no. 3, pp. 325–362, 1952. doi: doi.org/10.1680/ipeds.1952.11259.

[26] L. Farina and S. Rinaldi, *Positive linear systems: theory and applications*. John Wiley & Sons, 2000, vol. 50. ISBN 0471384569

[27] G. Bianchin and F. Pasqualetti, "Gramian-based optimization for the analysis and control of traffic networks," *IEEE Transactions on Intelligent Transportation Systems*, vol. 21, no. 7, pp. 3013–3024, 2020. doi: 10.1109/TITS.2019.2922900.

[28] G. Como, K. Savla, D. Acemoglu, M. A. Dahleh, and E. Frazzoli, "Robust distributed routing in dynamical networks - part I: Locally responsive policies and weak resilience," *IEEE Transactions on Automatic Control*, vol. 58, no. 2, pp. 317–332, 2013. doi: 10.1109/tac.2012.2209951.

[29] D. Branston, "Link capacity functions: A review," *Transportation research*, vol. 10, no. 4, pp. 223–236, 1976. doi: 10.1016/0041-1647(76)90055-1.

[30] J. Hofbauer and K. Sigmund, "Evolutionary game dynamics," *Bulletin of the American mathematical society*, vol. 40, no. 4, pp. 479–519, 2003. doi: 10.1090/s0273-0979-03-00988-1.

[31] B. Drighes, W. Krichene, and A. Bayen, "Stability of nash equilibria in the congestion game under replicator dynamics," in *IEEE Conf. on Decision and Control*, 2014. doi: 10.1109/CDC.2014.7039679. pp. 1923–1929.

[32] E. Hopkins, "A note on best response dynamics," *Games and Economic Behavior*, vol. 29, no. 1, pp. 138 – 150, 1999. doi: 10.1006/game.1997.0636.

[33] W. H. Sandholm, "Population games and deterministic evolutionary dynamics," in *Handbook of game theory with economic applications*, 2015, vol. 4, pp. 703–778. ISBN 978-0-444-53766-9

[34] A. Haurie and P. Marcotte, "On the relationship between nash—cournot and wardrop equilibria," *Networks*, vol. 15, no. 3, pp. 295–308, 1985. doi: 10.1002/net.3230150303.

[35] R. K. Ahuja, T. L. Magnanti, and J. B. Orlin, *Network flows*. New Jersey: Prentice Hall, 1988. ISBN 013617549X

[36] J. A. Jacquez and C. P. Simon, "Qualitative theory of compartmental systems," *Siam Review*, vol. 35, no. 1, pp. 43–79, 1993. doi: 10.1137/1035003.

[37] R. J. Plemmons, "M-matrix characterizations. I—nonsingular M-matrices," *Linear Algebra and its applications*, vol. 18, no. 2, pp. 175–188, 1977. doi: 10.1016/0024-3795(77)90073-8.

[38] H. K. Khalil, *Nonlinear Systems*, 2nd ed. Prentice Hall, 1995. ISBN 0132280248